Eduvest – Journal of Universal Studies
Volume 6 Number 6, June, 2026
p- ISSN 2775-3735- e-ISSN 27753727

# Development of a Responsive Airbag Hardware Mechanism for Fall Mitigation and Injury Reduction in the Elderly

**Sigit Indriyanto*, Willy Anugrah Cahyadi, Husneni Mukhtar, Muhammad Fasha Aqillah, Suto Setiyadi**
Universitas Telkom, Indonesia
Email: sigitindriyanto@student.telkomuniversity.ac.id*, waczze@telkomuniversity.ac.id, husnenimukhtar@telkomuniversity.ac.id, mfashaa@student.telkomuniversity.ac.id, sutosetiyadisod@telkomuniversity.ac.id

***Keywords:***
Wearable Airbag;
Fall Detection;
Elderly Safety;
IMU Sensor;
Servo Trigger

**ABSTRACT**

Falls pose a significant risk to elderly individuals and often result in serious injuries due to the lack of immediate protective mechanisms. Therefore, a real-time protective system is needed to reduce the impact of falls. The research aims to develop a wearable airbag vest system that integrates real-time fall detection with a servo-based mechanical triggering mechanism for rapid airbag deployment. The system utilized an IMU sensor to monitor body motion and orientation, a microcontroller to process detection logic, and a servo motor to activate a $CO_2$ inflator through a spherical buckle mechanism. Performance evaluation was conducted to assess IMU accuracy and airbag inflation response. The IMU demonstrated an average orientation error below 2% for yaw, pitch, and roll compared to an inclinometer reference. Inflation tests showed a servo current peak of 1200–2000 mA, with the airbag reaching peak pressure within 1.2–2.5 seconds after triggering, achieving pressure levels between 85 and 120 psi. The proposed servo-based triggering mechanism provides sufficient responsiveness and reliability for wearable fall protection applications.

## INTRODUCTION

Falls are one of the primary causes of serious injury among elderly individuals, frequently leading to fractures, reduced mobility, and long-term health complications (Nooruddin et al., 2022; Song et al., 2022). The risk of falling increases with age due to physiological factors such as decreased balance control, muscle weakness, and slower reaction time (Suprapto et al., 2024). In many cases, fall-related injuries occur not because of the fall itself, but due to the impact forces experienced during ground contact, particularly at the hip and upper body regions (Aravind et al., 2024; Nadee & Chamnongthai, 2015).

Most existing fall detection systems focus on post-fall monitoring and emergency notification, such as wearable alarms or smartphone-based detection, which do not provide physical protection at the moment of impact (Gizela et al., 2024; Usmani et al., 2021). As a result, these systems are limited in their ability to mitigate injury severity. To address this limitation, wearable airbag systems have been introduced as an active protection approach, capable of deploying cushioning structures around vulnerable body parts during a fall (Patra & Bandyopadhyay, 2025). However, current wearable airbag designs often rely on complex

triggering mechanisms, high energy inflators, or bulky actuators, which can reduce wearability, increase power consumption, and limit practical implementation (S. Kim & Kim, 2023).

Therefore, this study aims to develop a wearable airbag vest system that integrates real-time fall detection using an IMU sensor with a simple, low-power servo-based mechanical triggering mechanism for rapid airbag deployment (Semwal et al., 2023). The primary objective is to design and evaluate a responsive hardware mechanism capable of reducing impact forces during falls in elderly users.

The benefits of this research are twofold. First, it provides a practical and effective fall mitigation solution that directly reduces injury risk by absorbing impact energy, thereby improving the safety and quality of life for the elderly. Second, the proposed system offers a more feasible and energy-efficient alternative to existing wearable airbag designs, potentially increasing user compliance and enabling broader adoption in daily life due to its mechanical simplicity and lower power requirements.

This paper presents the development and experimental evaluation of a servo-driven wearable airbag vest that integrates IMU based fall detection with a mechanical inflator trigger mechanism. The proposed system emphasizes mechanical simplicity, actuator feasibility, and fast deployment response. Experimental results demonstrate that the servo actuator can reliably release low and medium stiffness spring mechanisms, while inflation tests show that the airbag reaches peak pressure within 1.2–2.5 s after trigger activation. These results indicate that a compact electromechanical triggering approach can provide an effective and practical solution for mitigating fall- related injuries in elderly users.

## METHOD

### System Design

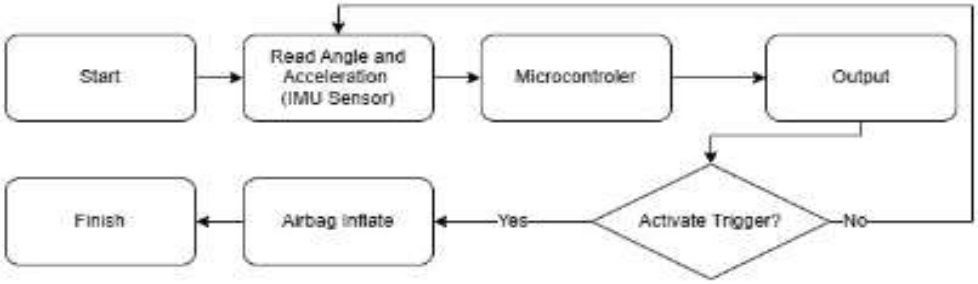


**Figure. 1. System Flowchart**
Source: Author's documentation, 2025

The flowchart describes the operational sequence of the airbag vest system from initialization to completion. The process begins with system startup, during which all components are initialized and prepared for operation. The IMU sensor then continuously measures acceleration and orientation data, including pitch, roll, and yaw angles, which are processed by the microcontroller to assess the user's motion state. Based on this analysis, the system evaluates whether predefined threshold conditions related to impact or fall characteristics are exceeded. If the conditions are not met, the system continues monitoring in real time. When a potential fall or impact is detected, the trigger mechanism is activated, initiating rapid airbag inflation to protect the user. After deployment, a notification is sent to

inform relevant parties of the activation, and the process concludes by resetting or terminating the system. This workflow enables reliable fall detection, timely airbag deployment, and effective user safety monitoring.

## Hardware Design

The vest used in this study is a motorcycle safety vest equipped with an integrated airbag system and a 12 g $CO_2$ inflator to ensure rapid airbag deployment. This system is designed to protect the user from impact during forward and backward falls. The hardware configuration consists of a WitMotion WT61PC-TTL IMU sensor, an Arduino Nano as the main controller, and a servo motor functioning as an actuator for the inflator mechanism.

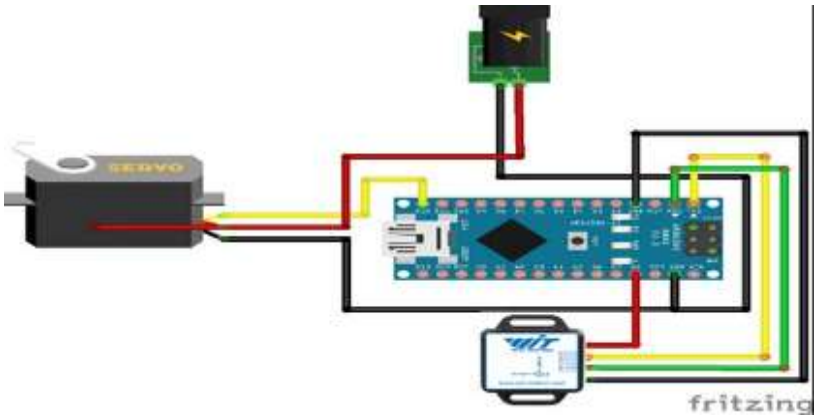


**Figure 2. Hardware Configuration (IMU, Arduino Nano, Servo Motor)**
Source: Author's documentation, 2025

## System Schematic

The IMU sensor is mounted on the upper back area of the vest, corresponding to the spinal axis, to provide stable measurements without restricting user movement (Ade et al., 2016). The controller unit and servo motor are positioned on the front left side of the vest, where the servo is mechanically connected to the inflator trigger using a carabiner for ease of use. The inflator operates by releasing a locking mechanism that drives a spring-loaded needle to puncture the $CO_2$ cartridge, allowing high pressure gas to rapidly inflate the airbag (Ade et al., 2016).


**Figure 3. Airbag Vest Model**
Source: Author's documentation, 2025

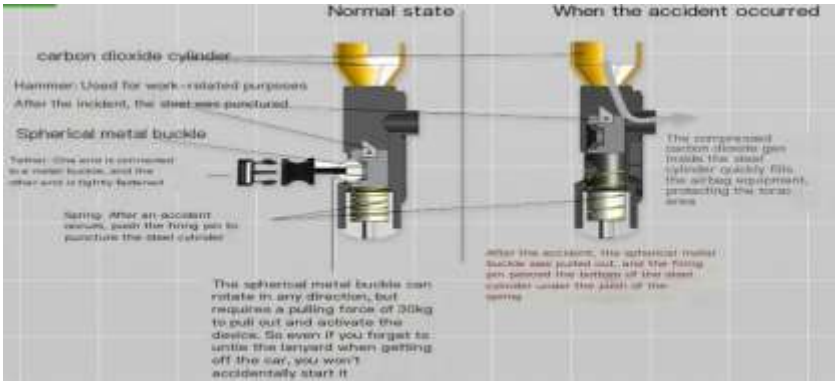


**Figure 4. Inflator Trigger Mechanism**

Source: Author's documentation, 2025

**Data Collecting Scenario**

The data collection process plays a crucial role in the development and validation of the airbag vest system by providing representative and reliable data from various fall and collision conditions. Key parameters affecting system performance are identified and categorized into input and output variables. The input parameters include impact speed derived from IMU acceleration data, impact angle, and user orientation expressed by pitch, roll, and yaw (Shi et al., 2009). The output parameters consist of airbag deployment time and inflation pressure, which indicate the responsiveness and protective effectiveness of the system (Song et al., 2022).

Data acquisition is carried out using an IMU sensor integrated with an Arduino-based controller for real-time data logging. The airbag vest prototype is mounted on crash test dummies and tested in a controlled environment to minimize external disturbances (Stewart, 2022). Various scenarios, including vertical falls, inclined impacts, and lateral or frontal collisions, are repeatedly simulated to ensure data robustness. The collected data are then organized, filtered, and normalized to ensure quality and consistency, forming a reliable dataset for subsequent system modeling and validation (M. Kim et al., 2019).

**Hardware Testing Scenario**

A test bench was developed to evaluate the gyroscope performance of the IMU sensor. The setup consists of two flat panels connected by hinges, enabling controlled angular rotation. An IMU sensor and an inclinometer, used as a reference for angular displacement, are mounted on the movable panel. By tilting the panel at predefined angles, the gyroscope measures angular velocity while the inclinometer provides the corresponding tilt angle (Bernardes & Viollet, 2022; Ling & Shabana, 2021). This configuration allows direct comparison between gyroscope-derived data and reference measurements to assess accuracy, drift, and responsiveness (Hasan, 2017).

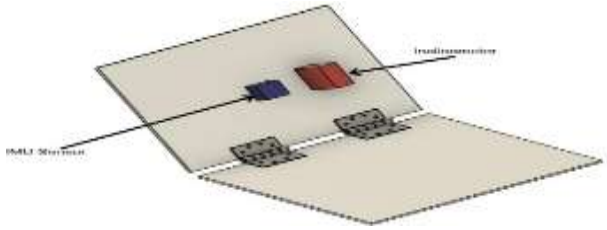

**Figure 2. IMU Sensor Angle Test Bench**

Source: Author's documentation, 2025

Accelerometer performance is evaluated through a free fall test in which the IMU sensor is dropped from heights of 50 cm and 70 cm. To examine the influence of surface conditions, tests are conducted on both hard and soft surfaces, the latter represented by an inflatable cushion. The recorded acceleration data are analyzed to evaluate peak impact forces and shock characteristics, which are essential for validating the accelerometer's reliability in fall detection and wearable protection applications (Korendiy et al., 2022).

A dedicated test bench is developed to evaluate the pulling force produced by the servo motor. The setup consists of a servo motor equipped with a servo arm connected to a wire, with the opposite end attached to a digital weight scale. As the servo rotates, the servo arm generates a horizontal pulling force that is recorded in real time. This configuration enables the measurement of the maximum pulling force under specific operating conditions, which is essential for mechanical actuation tasks such as trigger activation in an airbag vest system.

**Data Collecting Scenario**

The data collection process plays a crucial role in the development and validation of the airbag vest system by

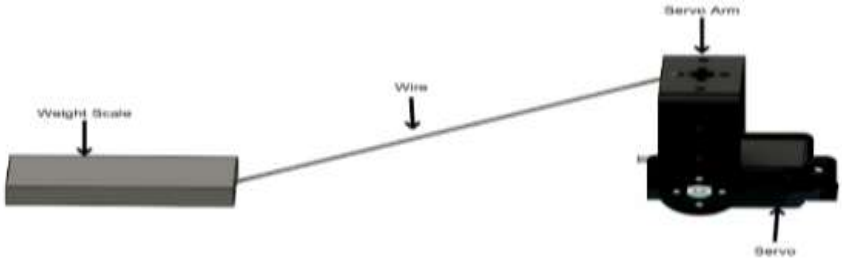


**Figure 3. Servo Pull Test Scenario**

Source: Author's documentation, 2025

The test bench further enables estimation of the mechanical torque generated by the servo motor using measured parameters, including pulling force $F$, servo arm length $r$, and the angle $\theta$between the servo arm and the pulling direction. The torque $\tau$is calculated using

$$\tau = F \cdot r \cdot sin\,(\theta) \qquad (1)$$

where $F$is obtained from the load cell output. When the weight scale provides mass readings $m$, the pulling force is calculated using

$$F = m \cdot g \qquad (2)$$

with $g = 9.81\ \text{m/s}^2$ (Hasan, 2017). The load cell is interfaced with an HX711 module and calibrated using standard weights. In addition, the servo's voltage and current are measured simultaneously during the pulling test to estimate power consumption, ensuring the suitability of the servo for integration into the overall system.

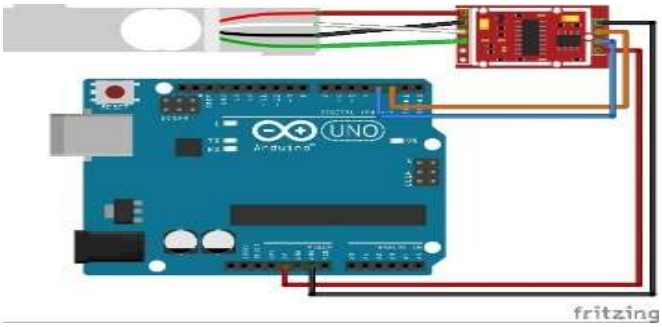


**Figure 4. HX711 Load Cell Schematic**

Source: Adapted from HX711 Datasheet (SparkFun, 2015) / Author's design, 2025

An inflation test is performed to evaluate a $CO_2$ inflator actuated by a spherical metal buckle mechanism, with the objective of identifying the optimal spring configuration capable of generating sufficient force to puncture the $CO_2$ cartridge and initiate rapid airbag inflation. The inflator utilizes a spring-loaded firing pin that converts stored elastic energy into kinetic energy upon release to pierce the cartridge seal.

Several springs with different stiffness values and free lengths are evaluated by replacing the original spring. The spring force is calculated using Hooke's Law,

$$F = k \cdot x \qquad (3)$$

where $k$is the spring constant (N/m) and $x$is the compression distance (m). For helical round-wire springs, the spring constant is given by

$$k = \frac{Gd^4}{8D^3N} \qquad (4)$$

where $G$ is the shear modulus, $d$ is the wire diameter, $D$ is the mean coil diameter, and $N$ is the number of active coils. For flat or shaped-wire springs, the stiffness is estimated using

$$k = \frac{Ebt^3}{4L^3} \qquad (5)$$

where $E$is the elastic modulus, $b$is the spring width, $t$is the thickness, and $L$ is the spring length.

All geometric parameters are obtained from manufacturer specifications or direct measurements. Each spring is tested for consistent puncture activation and complete gas release, and the results are compared to determine the most reliable configuration. The valve bracket performance is also evaluated using a servo motor, with successful operation defined by smooth and reliable valve opening and closing.

## RESULT AND DISCUSSION

### IMU Sensor Test Result

The first stage of testing evaluates the accuracy of the IMU sensor's angle measurements. Pitch, roll, and yaw outputs are compared with reference readings obtained from a protractor and an inclinometer mounted on the test bench. The test bench is tilted to predefined angles ranging from 0° to 90° in 10° increments. The same procedure is applied to all three axes to ensure consistency. The resulting measurements for yaw, pitch, and roll are then analyzed and compared with the reference values

**Table 1. IMU Sensor Angle Test Result**

| Protractor ($^o$) | Yaw | | Pitch | | Roll | |
|---|---|---|---|---|---|---|
| | ***Inclinometer ($^o$)*** | ***IMU Sensor ($^o$)*** | ***Inclinometer ($^o$)*** | ***IMU Sensor ($^o$)*** | ***Inclinometer ($^o$)*** | ***IMU Sensor ($^o$)*** |
| 0 | 0.12 | 0.06 | 0.03 | 0 | 0.07 | 0.03 |
| 10 | 10.17 | 10.02 | 10.76 | 10.45 | 10.03 | 10.25 |
| 20 | 19.45 | 19.73 | 20.13 | 20.64 | 20.59 | 20.01 |
| 30 | 29.77 | 30.04 | 30.35 | 29.92 | 29.29 | 30.32 |
| 40 | 40.63 | 40.03 | 40.78 | 40.04 | 39.23 | 40.02 |
| 50 | 49.83 | 50.1 | 49.98 | 50.14 | 49.39 | 49.98 |
| 60 | 59.58 | 60.01 | 59.62 | 60.33 | 58.2 | 59.59 |
| 70 | 68.64 | 70.07 | 69.82 | 70.17 | 68.62 | 69.25 |
| 80 | 78.56 | 79.96 | 79.62 | 79.99 | 77.73 | 79.49 |
| 90 | 89.94 | 90.12 | 89.9 | 88.14 | 88.67 | 89.14 |

Source: Author's test data, 2025

A drop test was performed to evaluate the accelerometer response to sudden changes in acceleration along the X, Y, and Z axes (Ibrahim et al., 2023). The sensor was released from a fixed height onto different surface types, while acceleration data were recorded in real time using a microcontroller. This test assessed the sensor's sensitivity, response time, and robustness under high dynamic conditions. The resulting data provide insight into the accelerometer's effectiveness in detecting sudden motion and impact events.

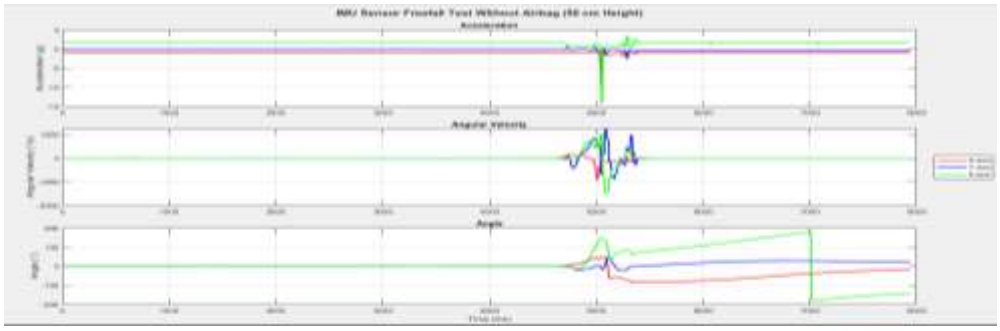

**Figure 5. IMU Sensor Fall Test Without Airbag (50cm Height)**

Source: Author's test data, 2025

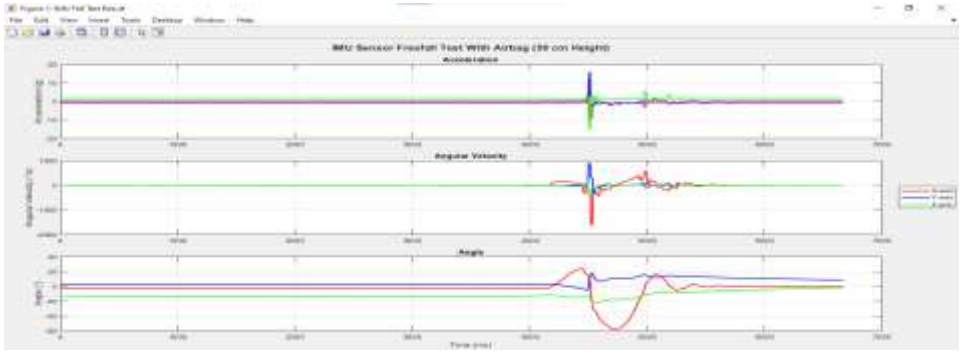

**Figure 6 . IMU Sensor Fall Test With Airbag (50cm Height)**

Source: Author's test data, 2025

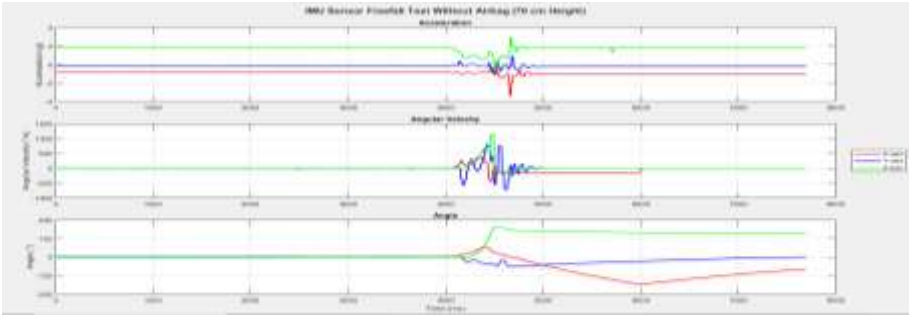

**Figure 7. IMU Sensor Fall Test Without Airbag (70cm Height)**
Source: Author's test data, 2025

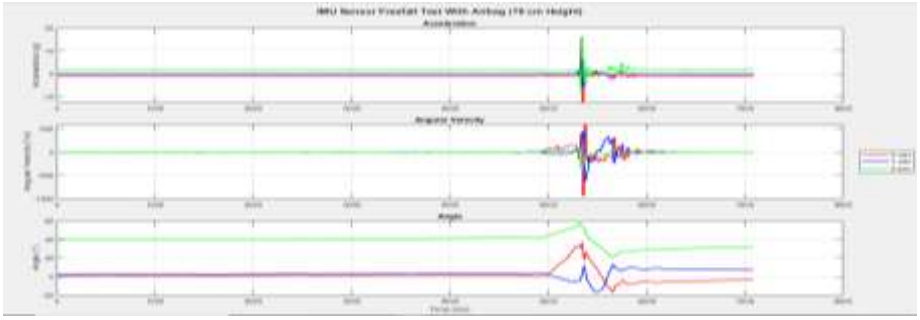

**Figure 8. IMU Sensor Fall Test With Airbag (70cm Height)**
Source: Author's test data, 2025

In the without airbag condition, acceleration signals exhibit sharp impact peaks that increase with drop height, indicating higher impact energy at greater heights. Angular velocity and orientation responses show large fluctuations and permanent deviations, reflecting significant rotational disturbances and reduced post impact stability.

In contrast, the with airbag condition demonstrates reduced peak acceleration and extended impact duration, indicating effective energy absorption. Angular velocity fluctuations are suppressed, and orientation deviations are smaller with improved post impact stability. Overall, the results confirm that the airbag significantly mitigates impact forces and rotational motion, supporting its effectiveness for wearable fall protection systems.

**Servo Pull Test Result**

This section presents the performance evaluation of three servo motors under tensile loading conditions, focusing on their electrical and mechanical responses, including supply voltage behavior, current consumption, and maximum pulling force.

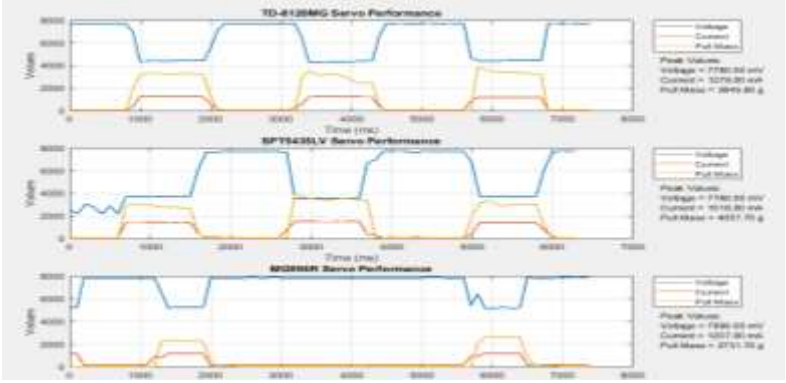

**Figure 9. Servo Pull Test Result**
Source: Author's test data, 2025

The TD-8120MG servo exhibits a noticeable voltage drop from 7.7 V under load, accompanied by an increase in current up to 1279 mA, which is characteristic of DC motors operating near high torque conditions. Despite this voltage reduction, the servo achieves a maximum pulling force of 3845.8 g, indicating adequate mechanical efficiency. The SPT5435LV servo shows a similar voltage drop but draws a higher peak current of 1518 mA and produces the highest pulling force of 4057.7 g. This result suggests superior force output capability and more effective power to torque conversion, possibly due to a more responsive internal control mechanism.

In contrast, the MG996R servo demonstrates the lowest performance, with a peak current of 1207 mA and a maximum pulling force of only 2731.7 g, despite maintaining a relatively stable supply voltage. This behavior reflects inherent torque limitations and reduced mechanical efficiency. Overall, the results reveal a consistent relationship between voltage drop and current increase during high-load operation, while highlighting significant differences in force capability among the servos. Among the tested units, the SPT5435LV provides the best pulling performance, whereas the MG996R shows the lowest suitability for high-load actuation, emphasizing the importance of actuator selection based on force and power requirements.

**Airbag Vest Test Result**

The final test is airbag vest test. In this experiment, the IMU sensor was mounted on the upper back region of the vest to ensure measurement stability and minimize interference from airbag deployment. The inflator trigger mechanism employed a servo motor positioned at the lower section of the inflator, while the Arduino Nano and battery were installed on the left side of the vest as the control unit.

**Figure 10. Airbag Vest Result**
Source: Author's test data, 2025

The airbag vest was tested by dropping the vest mounted on a mannequin. Inflation performance was evaluated by measuring the time required to reach maximum airbag pressure using a pressure sensor installed near the inflator, which was connected to the vest through a brass tube.

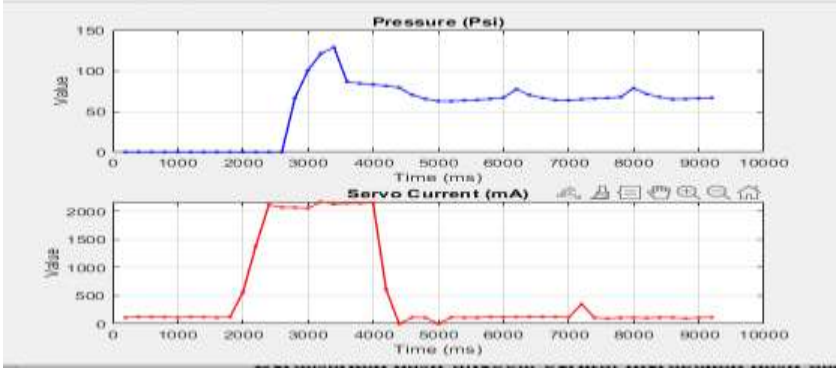


**Figure 11 Pressure and Servo Current Value Comparison on Inflator**

Source: Author's test data, 2025

Based on the time-response characteristics, servo activation is indicated by a sharp rise in current at around 2000 ms, corresponding to the application of maximum torque to release the inflator mechanism. The airbag pressure then increases rapidly and reaches a peak value of 120 psi at 3200–3300 ms. This result indicates an inflation response time of 1.2–1.3 s from trigger activation to peak pressure, confirming that the servo-driven inflator mechanism provides a sufficiently fast response for protective applications.

To assess the effectiveness of the protective vest in reducing impact forces during falls, controlled drop tests were conducted in four directions: left, front, right, and back. Each scenario was evaluated under two conditions, with and without the vest, to enable direct comparison of sensor responses. Accelerometer and gyroscope data were analyzed to examine changes in linear acceleration, angular velocity, and post-impact stability. Analysis of peak values and signal behavior provides insight into the vest's ability to absorb impact energy and reduce dynamic forces during fall events.

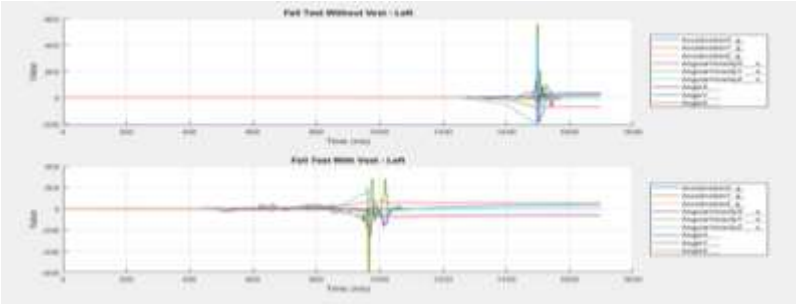

**Figure 12. Airbag Fall Test Result (Left)**

Source: Author's test data, 2025

During the left-side fall test without the protective vest, the accelerometer data exhibited a sharp increase in acceleration at the moment of impact, particularly on the Z-axis, which recorded a prominent peak. This peak was followed by multiple oscillations, indicating that the sensor experienced rebound effects after contacting the ground. The gyroscope data showed significant variations on all three rotational axes, suggesting abrupt and uncontrolled body rotation during the fall. When the test was repeated with the vest, the acceleration peaks were noticeably reduced, and the post-impact oscillations dissipated more rapidly. This indicates that the vest absorbed a portion of the impact energy, reducing the impulsive force transmitted to the sensor and stabilizing the body's motion after the collision

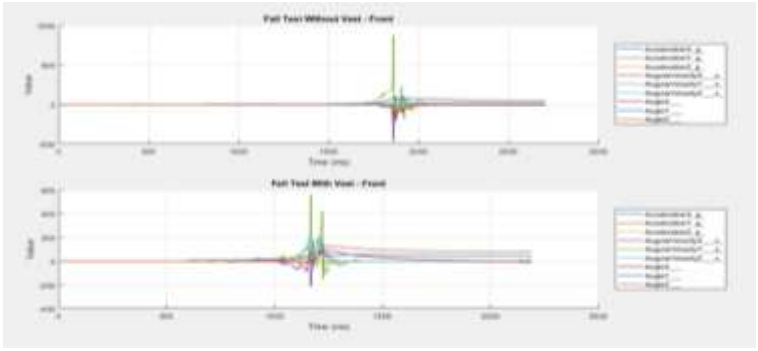

**Figure 13. Airbag Fall Test Result (Forward)**
Source: Author's test data, 2025

In the forward fall without the vest, the accelerometer recorded the highest impact peaks, particularly along the Z-axis, accompanied by large gyroscope fluctuations indicating severe rotational motion. When the vest was used, acceleration peaks were significantly reduced and rotational responses became more controlled. These results demonstrate that the vest attenuated forward impact forces and limited excessive rotational movement, thereby reducing injury risk to the frontal body region.

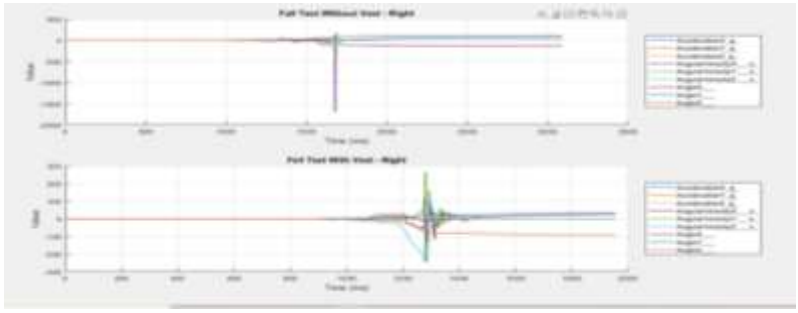

**Figure 17. Airbag Fall Test Result (Right)**
Source: Author's test data, 2025

For the right-side fall test without the vest, the sensor recorded an exceptionally large negative acceleration peak, indicating one of the hardest impacts among all scenarios. The gyroscope readings also displayed abrupt rotational changes, and the post-impact oscillations were longer and more pronounced due to the lack of damping. In contrast, when the vest was used, the maximum acceleration values decreased considerably, and the oscillations became smaller and decayed more quickly. This demonstrates the vest's effectiveness in attenuating lateral impact forces and limiting the transfer of energy to the body during side falls

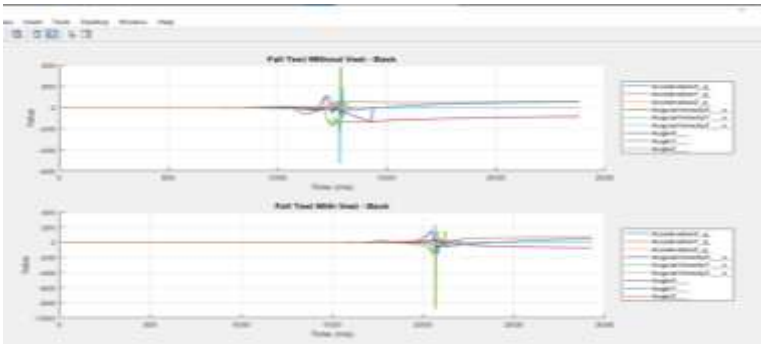

**Figure 14. Airbag Fall Test Result (Backward)**
Source: Author's test data, 2025

accelerometer recorded high impact peaks followed by prolonged oscillations, while the gyroscope data showed abrupt and potentially hazardous rotational motions. When the vest was worn, both acceleration peaks and oscillations were significantly reduced, and rotational responses became more stable, indicating effective impact damping and improved body stability. Thus, the results across all fall directions show that the absence of the vest leads to higher impact forces and more extreme dynamic responses. In contrast, the use of the protective vest consistently reduces peak acceleration, shortens stabilization time, and suppresses excessive rotational motion, confirming its effectiveness as an energy-absorbing protective system

## CONCLUSION

Based on the design and comprehensive testing of the airbag vest system, the results confirm that the IMU sensor provides reliable fall detection, while the accelerometer captures high-impact events. The voltage, current, and pressure sensors demonstrate accurate and stable measurements, ensuring dependable system monitoring. Among the tested actuators, the SPT5435LV servo delivers the highest pulling force and is most suitable for inflator triggering, while selected spring configurations reliably activate the CO2 inflator. System level and comparative fall tests show rapid airbag deployment and a significant reduction in impact acceleration when the vest is used, validating the effectiveness of the proposed wearable airbag system in mitigating fall-related injuries for elderly users. Despite the promising results, several limitations should be addressed in future research. Future work should incorporate machine learning algorithms to better distinguish falls from daily activities and reduce false positives. The prototype also needs miniaturization and weight reduction using smaller servos, compact $CO_2$ cartridges, and flexible PCBs to improve wearability. Researchers should explore reusable or multi-stage inflation systems to lower costs and environmental impact. Clinical trials involving elderly participants are essential to validate real-world performance, while wireless connectivity and smartphone applications could enable real-time alerts and health monitoring. Additional testing is needed for complex fall scenarios such as tripping or slipping on stairs. Energy harvesting technologies could extend battery life, and direct comparisons with commercial products like HipGuard or Helite would help benchmark performance. Finally, selecting low-cost components and optimizing for affordable mass production will make the system accessible to elderly users in low-resource settings.

## REFERENCE


Ade, N., Stämpfli, R., & Schmitt, K.-U. (2016). Evaluating airbag safety vests for equestrian sports. *Journal of Testing and Evaluation*, *44*(6), 2387–2395.

Aravind, G., Kiran, V. V., Sukumar, V. M., & Suhasini, P. S. (2024). Fall Detection and Protection by Airbag System. *2024 International Conference on Expert Clouds and Applications (ICOECA)*, 505–510.

Bernardes, E., & Viollet, S. (2022). Quaternion to Euler angles conversion: A direct, general and computationally efficient method. *Plos One*, *17*(11), e0276302.

Gizela, B. A., Almira, A. S., & Pratiwi, W. R. (2024). Prevalensi cedera akibat jatuh pada kelompok lanjut usia dan pra-lanjut usia. *MJS Medical Journal of Soeradji*, *1*(1), 46–60.

Hasan, D. (2017). Calculation of angular velocity, angular acceleration and torque of two

common point rigid bodies using IMU. *Journal of Applied and Physical Sciences*.
Ibrahim, M., Shawish, S., Aldroubi, S., Dawoud, A., & Abdin, W. (2023). Airbag protection and alerting system for elderly people. *Applied Sciences*, *13*(16), 9354.
Kim, M., Cho, J., Lee, S., & Jung, Y. (2019). IMU sensor-based hand gesture recognition for human-machine interfaces. *Sensors*, *19*(18), 3827.
Kim, S., & Kim, M. (2023). Rotation representations and their conversions. *Ieee Access*, *11*, 6682–6699.
Korendiy, V., Kachur, O., Gurskyi, V., & Krot, P. (2022). Studying the influence of the impact gap value on the average translational speed of the wheeled vibration-driven robot. *Engineering Proceedings*, *24*(1), 25.
Ling, H., & Shabana, A. A. (2021). Euler angles and numerical representation of the railroad track geometry. *Acta Mechanica*, *232*(8), 3121–3139.
Nadee, C., & Chamnongthai, K. (2015). Ultrasonic array sensors for monitoring of human fall detection. *2015 12th International Conference on Electrical Engineering/Electronics, Computer, Telecommunications and Information Technology (ECTI-CON)*, 1–4.
Nooruddin, S., Islam, M. M., Sharna, F. A., Alhetari, H., & Kabir, M. N. (2022). Sensor-based fall detection systems: a review. *Journal of Ambient Intelligence and Humanized Computing*, *13*(5), 2735–2751.
Patra, B., & Bandyopadhyay, S. (2025). An analytical study of Euler angle and Rodrigues parameter representations of geometrically and establishing the relations between these. *Robotica*, *43*(1), 163–193.
Semwal, V. B., Kumar, A., Nargesh, P., & Soni, V. (2023). Tracking of fall detection using IMU sensor: An IoHT application. *Machine Learning, Image Processing, Network Security and Data Sciences: Select Proceedings of 3rd International Conference on MIND 2021*, 815–826.
Shi, G., Chan, C. S., Li, W. J., Leung, K.-S., Zou, Y., & Jin, Y. (2009). Mobile human airbag system for fall protection using MEMS sensors and embedded SVM classifier. *IEEE Sensors Journal*, *9*(5), 495–503.
Song, Z., Ou, J., Shu, L., Hu, G., Wu, S., Xu, X., & Chen, Z. (2022). Fall risk assessment for the elderly based on weak foot features of wearable plantar pressure. *IEEE Transactions on Neural Systems and Rehabilitation Engineering*, *30*, 1060–1070.
Stewart, S. L. (2022). *Safely Covered or Dangerously Exposed: Analyzing the Safety Vest Code of Compliance*.
Suprapto, S. S., Kusuma, V. A., Firdaus, A. A., Putra, W. H., & Yuniar, R. J. (2024). Design and build an airbag system for elderly fall protection using the MPU6050 sensor module. *International Journal of Reconfigurable and Embedded Systems (IJRES)*, *111*, 111–116.
Usmani, S., Saboor, A., Haris, M., Khan, M. A., & Park, H. (2021). Latest research trends in fall detection and prevention using machine learning: A systematic review. *Sensors*, *21*(15), 5134.